OPTIMAL SCHEDULING MODEL OF A VIRTUAL POWER PLANT BASED ON ROBUST OPTIMIZATION WITH ADDITIONAL MOMENTUM TO IMPROVE THE PREDICTIVE OUTPUT OF BACK PROPAGATION NEURAL NETWORKS

Menglin Hou, Zhumei Luo[1,*], Xiaoxu Zhang[1], Shan Qing[1], Xiaohui Zhang[1]

[*1] Kunming University of Science and Technology, Kunming, 650093, China

[*] Corresponding author; E-mail: m15087088903@163.com

In response to energy shortages, uneven distribution, and severe pollution, the global energy structure is rapidly changing. In the dispatching of power systems, the coordinated planning and flexible regulation of virtual power plants play a crucial role. This paper proposes a multi-objective model considering economic efficiency and carbon emissions to study the scheduling of virtual power plants and the proportion of new energy installed capacity.

Firstly, the paper optimizes the power system load curve by implementing time-of-use pricing strategies, alleviating the additional pressure on installed capacity caused by demand differences during peak and off-peak periods. Secondly, an improved back propagation neural network method is employed to refine the robust interval, and by integrating feedback historical data, the adaptive robust control theory is enhanced, thereby improving the system's robustness and adaptability. Finally, through specific case analysis and scenario simulation, the paper finds that when the proportion of new energy in the system reaches 60%, it is possible to maximize economic efficiency and minimize carbon emissions while ensuring the stable operation of the virtual power plant.

Key words*: virtual power plant; improving back propagation neural networks; robust optimization; risk tolerance*

1. Introduction

In today's rapid industrialization, we are facing the severe challenge of the deteriorating global environment [1]. The energy industry, as one of the main sources of environmental pollution, has become the focus of global attention for its reform and transformation [2]. In particular, the electricity industry is at the center of this transformation storm. With the continuous expansion of the scale of renewable energy integration and the increasing penetration rate, the safe and stable operation of the power system is facing unprecedented tests. These tests mainly come from the uncertainty and volatility of renewable energy output, which requires the power system to improve its flexible regulation capabilities [3]. The emergence of Virtual Power Plant (VPP) technology has effectively addressed the challenges brought by the integration of renewable energy into the grid by integrating distributed generation, energy storage systems (ESS), and dispatchable loads, and implementing coordinated control, enabling VPP to participate in the electricity market and ancillary services market

[4]. Therefore, research on virtual power plants is of profound significance for the future development of power systems and electricity markets.

To mitigate the impact of renewable energy on the stability of the power system, accurate prediction of its output has become a key task before grid connection [5]. Currently, research on the prediction of wind and photovoltaic (PV) power generation has received extensive attention. These predictions are usually based on different time scales and use machine learning methods to conduct ultra-short-term, short-term, medium-term, and long-term output power predictions according to numerical weather forecasts. Common machine learning methods include convolutional neural networks [6], long short-term memory networks [7], recurrent neural networks [8], etc. However, due to the less-than-ideal quality of input data or the limitations of the prediction models themselves, the accuracy of the prediction results is often limited, affecting the precise formulation of power system dispatch plans [9].

The integration of renewable energy in virtual power plants increases the difficulty of balancing supply and demand in the power system load. To reduce and quantify the operational risks of the system, scholars have proposed various methods [10]. For example, Huang and others have used probability theory to predict intervals of system output and load but did not fully consider the impact of factor mutations[11]. Zamani and others have used the PEM method to deal with the uncertainty of wind and PV[12]. Shabanzadeh and others have applied Second-Order Stochastic Dominance Constraints (SSDs) to cope with fluctuations in market prices[13]. Rahimiyan and others have used Robust Optimization (RO) models to solve the problem of uncertainty under different risk strategies in VPP[14]. Zhong Futan and others have analyzed the impact of wind and solar energy uncertainty on system stability based on robust optimization theory [15]. The mixed integer linear programming (MILP) model proposed by Shabanzadeh and others based on robust optimization theory can solve the problem of electricity market instability under day-ahead scheduling problems in VPP [16], while Baringo and others have studied the scheduling optimization of VPP in energy and electricity markets through the stochastic adaptive robust optimization method[17]. However, robust optimization theory may overly restrict the use of renewable energy to ensure the stable operation of the system.

As the main energy source in our daily life, the stability of the power system is crucial. However, excessive restrictions may lead to a reduction in energy utilization and cause energy waste. Therefore, this article proposes to optimize the power structure and increase the proportion and utilization of renewable energy on the premise of ensuring the stable operation of virtual power plants. We propose the following innovations:

(1) To refine the robust interval, we have improved the backpropagation neural network by introducing additional momentum to accurately simulate and predict wind and solar power generation, creating a prediction model with an accuracy of over 95%.

(2) We have constructed a virtual power plant model that includes wind power generation, photovoltaic power generation, hydroelectric power generation, classical thermal power generation, and energy storage systems, using the economic efficiency and carbon emissions of VPP as the objective function, and adjusting the robustness coefficient to analyze the impact of wind and solar integration on the system, reflecting the risk tolerance of VPP.

2. Structure of Virtual Power Plant

The virtual power plant is a complex system that consists of several key components: In-region power generation system: This refers to the various power generation sources located within a specific region. It includes wind power plants, photovoltaic (solar) power plants, hydroelectric power plants, and classical thermal power plants. Classical thermal power plants, such as coal or natural gas plants, and hydroelectric power plants have been well-developed and can be regulated conveniently and stably. However, wind power plants and photovoltaic power plants face challenges in effective regulation due to natural variability and technical constraints. Energy storage power plant: This component focuses on storing excess energy generated by the power generation system for later use. It includes different types of energy storage technologies such as pumped storage power plants, air compression power plants, and battery energy storage power plants [18]. These facilities play a vital role in balancing supply and demand by storing excess energy during periods of low demand and releasing it during peak demand periods. Home energy storage batteries: These batteries are carried by household appliances like electric vehicles, air conditioners, and emergency energy storage power supplies[19]. They provide a decentralized energy storage solution at the consumer level, allowing households to store excess energy generated by the power generation system or charge during off-peak hours. This stored energy can then be used to power household appliances or provide backup power during outages. Load: The load represents the electricity consumption from different sectors, including residential, industrial, public, and commercial, as shown in fig. 1.

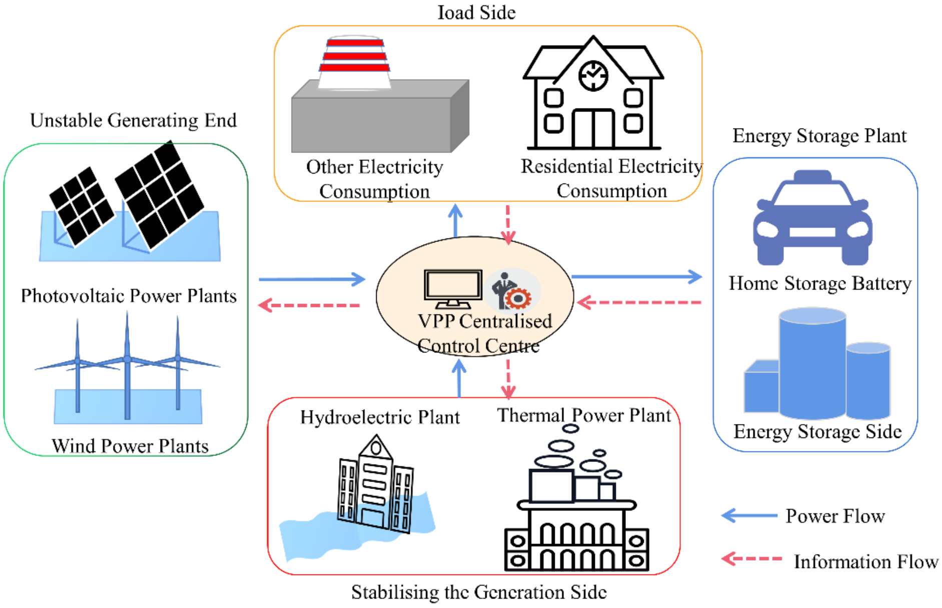

Figure 1. Basic structure of VPP

3. Scheduling model

The proposed approach in this paper aims to address the challenges posed by the volatility and intermittency of wind and solar energy. To achieve this, the operation of classical thermal and hydroelectric power plants is utilized to assist wind and photovoltaic power plants in smoothing their output curves. This helps to ensure that the generation system can meet the demand of electric power loads, even during intermittent periods of wind and solar energy. This approach also increases the utilization of clean and renewable energy from the unstable end of the system, thereby reducing environmental pollution. Moreover, energy storage plants and home storage batteries play a crucial role in storing excess power from the generation system. This stored power can be reused, increasing the utilization of renewable resources in virtual power plants. As a result, there is a reduction in the need for wind, solar, and water abandonment operations, leading to a more efficient and sustainable energy system. Additionally, the implementation of a demand response-based time-sharing tariff strategy on the load side is proposed. This strategy aims to improve user electricity behavior and smooth the load curve through peak and valley tariff differences. By offering incentives for users to participate in power market scheduling, such as using home energy storage batteries for peak shaving and valley power migration, users are encouraged to modify their electricity consumption patterns.

3.1. Objective function

In the virtual power plant dispatch optimization model proposed in this paper, the optimization objective is based on economic and carbon emission considerations for each system with different capacity ratios. The economic objective for wind and photovoltaic systems is determined by multiplying the grid-connected electricity at a specific moment (t) by the prevailing electricity price. For small-scale energy storage systems, the economic target is then determined by the amount of electricity stored and released and the difference in electricity price between the two moments. In contrast, the operating costs of wind, photovoltaic and hydroelectric systems are small compared to their construction costs. Therefore, their operating costs are not explicitly considered in the optimization model. Instead, the construction costs are spread over the operating hours and are considered as production costs. This approach reflects the long-term investment nature of these renewable energy systems. On the other hand, the costs of classical thermal power systems include operating costs and construction cost sharing.

By considering both economic and carbon emissions objectives, the optimization model aims to find the optimal dispatch strategy for the virtual power plant that minimizes costs while also reducing carbon emissions. This comprehensive approach takes into account the unique characteristics and costs associated with different energy generation systems within the virtual power plant.

Establishing a dual objective function for economic efficiency and carbon emissions,

$$\begin{cases} EB_{VPP} = \sum_{t=1}^{T} \{[E_{WP,t} + E_{PV,t} + E_{SRS,t} + E_{BES,t}] - C_{WP,t} - C_{PV,t} - C_{CTP,t}\} \\ CO_{VPP} = \sum_{t=1}^{T} \{[\lambda CO_{WP,t} + \lambda CO_{PV,t} + \lambda CO_{SRS,t} + \lambda CO_{BES,t}]\} \end{cases} \tag{1}$$

where EB_{VPP} denotes the economic efficiency of the virtual power plant, $E_{WP,t}$ denotes the benefits of the wind power system; $E_{PV,t}$ denotes the benefits of the photovoltaic power system $E_{SRS,t}$ denotes the benefits of the stabilisation control side; $E_{BES,t}$ denotes the benefits of the small storage system; $C_{PW,t}$ and $C_{PV,t}$ indicates construction costs for wind and photovoltaic power generation; $C_{CTP,t}$ denotes the costs of the stabilization side; λ denotes the carbon emission factor; CO_{VPP} denotes the total carbon emission from the virtual power plant; $CO_{WP,t}$ denotes the wind power generation system carbon emission; $CO_{PV,t}$ denotes the carbon emission of photovoltaic power generation system; $CO_{SRS,t}$ denotes carbon emissions from the stabilization control side; $CO_{BES,t}$ denotes carbon emissions from energy storage system.

3.2. Restrictive condition

The following constraints are placed on the components of the constituent systems to ensure safe and reliable operation of the virtual power plant:

3.2.1 Balancing supply and demand balance constraints in the power system

$$ER_{U,t} \le P_{WP,t}\theta_W + P_{PV,t}\theta_{PV} + P_{SRS,t}\theta_{SRS} + P_{BES,t}\theta_{BES} \le ER_{U,t} + ER_{BES,t} \quad (2)$$

$ER_{U,t}$ denotes the power demanded by the user at moment t; $P_{WP,t}$,$P_{PV,t}$,$P_{SRS,t}$,$P_{BES,t}$ denote, respectively, the real power of wind, *PV*, stable end, and small-scale storage at moment t; θ_{WP}, θ_{PV}, θ_{SRS}, θ_{BES}, denote the conversion efficiencies of wind, photovoltaic, stabilization, and home storage, respectively; and $ER_{BES,t}$ denotes the maximum power dissipation capacity of home storage at moment.

3.2.2 Unstable regulatory end constraints

In order to improve the utilization of renewable energy and to reduce the operation of wind and light abandonment, this paper makes the wind power generation system and photovoltaic power generation system to be in the state of maximum output at the present time, and its constraint is the climbing constraint of the unit itself.

$$0 \le P_{W,t-1} \pm \mu\Delta S_{WP} \le S_{WP,\max} \quad (3)$$

$$0 \le P_{PV,t-1} \pm \mu\Delta S_{PV} \le S_{PV,\max} \quad (4)$$

$\Delta S_{WP,PV}$ denotes the power variation limit values of wind and photovoltaic power generation.

3.2.3 Stabilizing the regulatory end of the constraint

$$P_{H,\min} \le P_{VPP_{\min},t} \le P_{H,t} + \Delta P_H \le P_{H,\max} \quad (5)$$

$$P_{TR,\min} \le P_{VPP_{\min},t} \le P_{TR,t} + \Delta P_{TR} \le P_{TR,\max} \quad (6)$$

In the equation, $P_{VPPmin,t}$ represents the minimum power output required by the system in the next phase; $P_{H,min/max}$ denotes the minimum and maximum limit of the hydropower plant's output power; $\Delta P_{H/TR}$ indicates the maximum ramping power of the hydrothermal power generating units. $P_{TR,min/max}$ represents the minimum and maximum power output limits of thermal power generation; P_t represents the current power output.

3.2.4 Large and small energy storage system constraints

$$0 \le S_{ES,t-1} \pm \mu\Delta S_{ES} \le S_{ES,\max} \quad (7)$$

$S_{ES,t-1}$ denotes the storage capacity of the energy storage system at the moment t-1, μ denotes the charging and discharging efficiency of the energy storage system, ΔS_{ES} denotes the limiting dissipation and output power of the energy storage system, and $S_{ES,max}$ denotes the maximum storage capacity of the energy storage system.

3.3. Optimized scheduling model

3.3.1 Robust optimization model

When the stabilizing and regulating end assumes the power load, the stability of the system is well ensured, but the classical thermal power generation system emits a large amount of gas during operation, causing serious pollution to the environment. When wind power and photovoltaic power generation take up the power load, its stochastic and intermittent characteristics will hinder the stable operation of the power system. In this paper, the robust stochastic optimization theory is used to change the wind and PV power output prediction results from accurate point prediction to short interval prediction, which reduces the impact of prediction errors on the virtual power plant, and improves the stability and accuracy of the virtual power plant in making the operation plan.

$$P_{WP,t} = P_{WP,t} + \alpha_t e_{WP,t} P_{WP,t} \qquad \alpha_t \in [-1,1] \tag{8}$$

$$P_{PV,t} = P_{PV,t} + \beta_t e_{PV,t} P_{PV,t} \qquad \beta_t \in [-1,1] \tag{9}$$

Estimated power interval range

$$P_{W,t} \in [(1-e_{W,t})P_{W,t} \qquad (1+e_{W,t})P_{W,t}] \tag{10}$$

$$P_{PV,t} \in [(1-e_{PV,t})P_{PV,t} \qquad (1+e_{PV,t})P_{PV,t}] \tag{11}$$

where $\tilde{P}_{W,t}$ and $\tilde{P}_{PV,t}$ are the uncertainty forms of wind and photovoltaic power generation, respectively; $e_{W,t}$ and $e_{PV,t}$ are the error coefficients of the prediction results of wind and photovoltaic power generation, respectively.

Eq.(1) is converted to the following inequality constraint:

$$ER_{U,t} \le P_{W,t}(1-\lambda_W) + P_{PV,t}(1-\lambda_{PV}) + P_{SRS,t}\theta_{SRS} + P_{BES,t}\theta_{BES} \tag{12}$$

$$P_{W,t}(1+\lambda_W) + P_{PV,t}(1+\lambda_{PV}) + P_{SRS,t}\theta_{SRS} + P_{BES,t}\theta_{BES} \le ER_{U,t} + ER_{BES,t} \tag{13}$$

where λ_{WP} and λ_{PV} denote the maximum deviation from the predicted results for WP and PV.

When optimizing scheduling using robust optimization theory, the precision of the uncertainty set has a significant impact on the results. However, a finely detailed uncertainty set increases the complexity of the model. To address the issue of a model being too complex to solve conveniently, this paper employs an improved Back Propagation (BP) neural network with additional momentum for power output prediction to refine the uncertainty set.

3.3.2 The modified Back Propagation neural network with additional momentum

Wind and photovoltaic power generation are subject to various factors, resulting in significant volatility and randomness. When these two sources of unstable power supply electricity to the VPP system, it poses a high risk to the system's stable operation. Hence, there is a pressing need for more precise forecasts of wind and solar power output. These forecasts are essential to provide reliable data for the VPP system, enabling it to formulate accurate output plans in advance. By comparing BPNN, RBF1, RBF2, PNN, GRNN, BPNN, which has the highest accuracy, is selected as the base method for this study [20].

Back propagation neural networks are a high-precision prediction method, which consists of an input layer, a hidden layer and an output layer. In the forward transmission process, the input signal is processed layer by layer starting from the input layer, passing through the hidden layer, and finally arriving at the output layer, whose topology is shown in fig. 2.

Although BPNN has better accuracy, it does not take into account the accumulation of previous experience and the learning process converges slowly. And it is easy to fall into local minima, which affects the prediction accuracy. Therefore, in this paper, this problem is solved by using an additional momentum method, and the weight learning formula for the additional momentum method is [21].

$$\omega(k) = \omega(k-1) + \Delta\omega(k) + a[\omega(k-1) - \omega(k-2)] \tag{14}$$

Where weights when $\omega(k), \omega(k-1), \omega(k-2)$ is k,k-1,k-2, a is the momentum learning rate.

Evaluation metrics play a crucial role in comparing the accuracy of different neural network models for predicting the output power of wind and solar energy. These metrics include Mean Bias (MBE), Root Mean Square Error (RMSE), Mean Absolute Error (MAE), and Regression Coefficient (R^2). The calculation of these metrics is carried out using eq.15 through 18 as follows:

$$MBE = \sum_{i=1}^{N} \frac{(k_i^M - k_i^P)}{N} \tag{15}$$

$$RMSE = \left\{ \sum_{i=1}^{N} \frac{(k_i^M - k_i^P)^2}{N} \right\}^{0.5} \tag{16}$$

$$MAE = \sum_{i=1}^{N} \frac{\left| k_i^M - k_i^P \right|}{N} \tag{17}$$

$$R^2 = \frac{\sum_{i=1}^{N} (k_i^M - \overline{\Delta k})^2 - \sum_{i=1}^{N} (k_i^M - \Delta k_i^P)^2}{\sum_{i=1}^{N} (k_i^M - \overline{\Delta k})^2} \tag{18}$$

where $k^{M/P}$ and N represent the predicted/actual output values and the number of data recorded for the project, respectively.

These metrics provide a quantified measure of the performance of neural network models, allowing for a comprehensive evaluation and aiding in the selection of the most accurate and reliable model. Values of MBE (Mean Bias Error), RMSE (Root Mean Square Error), and MAE (Mean Absolute Error) that approach zero indicate a high level of accuracy in the model. Furthermore, an R^2 value close to 1 further substantiates the model's accuracy. RMSE is particularly effective in identifying outliers with significant bias, while MAE offers a measure of the overall discrepancy from the mean. Collectively, these metrics provide a thorough assessment of the model's performance, ensuring that individual variations and anomalies are taken into account.

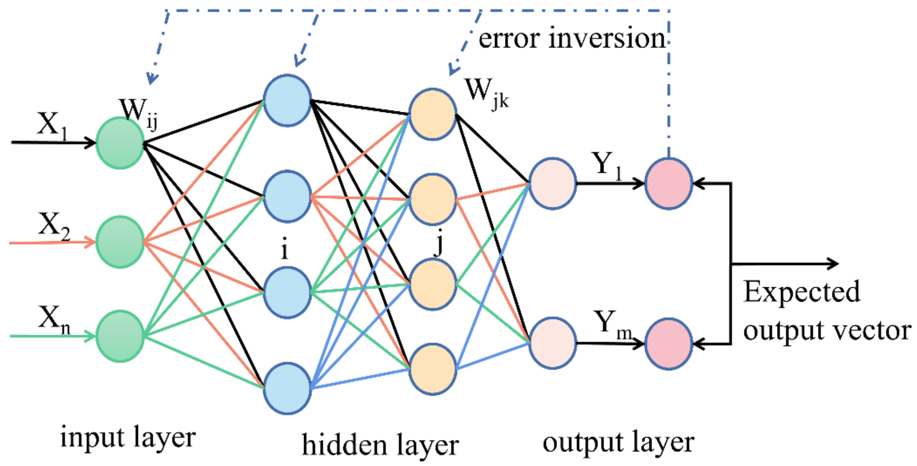

Figure 2. Topology diagram of BPNN

After successfully obtaining a more precise robust interval, the study employs Adaptive Robust Control (ARC) theory as the core theoretical framework. Through the learning process, it was discovered that the ARC control process lacks a feedback mechanism and that its decision-making primarily relies on operational data from previous periods. By introducing historical records and an analysis phase, the study enhances the learning and adaptive capabilities of ARC, significantly improving its optimization potential, as shown in fig. 3.

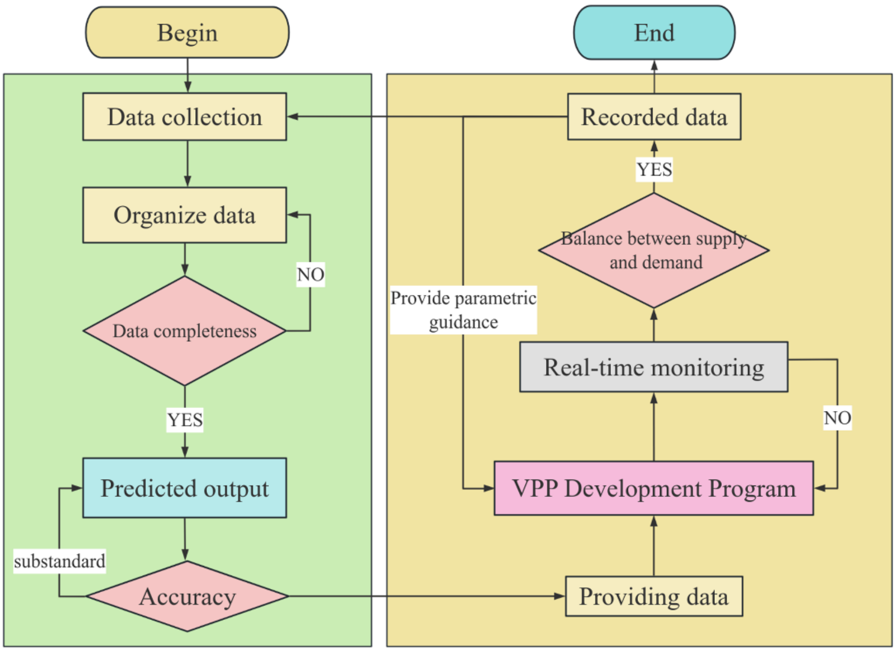

Figure 3. Virtual Power Plant Operation and Scheduling Flowchart

4. Example analysis

4.1. Basic data

Based on the above model analysis, the main parameters are shown in tab. 1.

Table 1. Basic data of the virtual power plant

Energy structure	Hydroelectricity	Thermal power station	Energy storage power plant	WP station	PV station
Installed capacity	700MW(140*5)	900MW(180*5)	500MW	500MW	110MW

4.2. Wind power and photovoltaic power output power forecasts

The wind and photovoltaic power stations have a stable grid-connected basis after three years of commissioning and trial operation after construction, and this paper takes the data of the last year of trial operation as the basis for simulating and predicting the output curves of the two plants in the future. The model is programmed by Matlab 2022a, and solved by Gurobi solver and B-P double hidden layer neural network. The training validation is done with data recorded every 10 minutes of unit operation and finally the prediction of the output curve of one of the wind turbines in the wind farm over a 24-hour period and one of the photovoltaic turbines in the photovoltaic farm over the time from sunrise (8:30) to sunset (18:30) is done. After selection and calculation, the optimal number of nodes in the hidden layer is set to 3, the optimal number of iterations is 10,000, the error threshold is 1e-6, and the learning rate is 0.005. After improvement, the momentum factor is increased to 0.95, the learning rate is changed to 0.05, and the confidence interval is set to the robust error coefficient of 0.95, which results in fig. 4 and fig. 5. It can be seen from the prediction result graphs that the prediction results before the optimization have multiple The accuracy of the predicted values is outside the 95% confidence interval, and after optimization, the predicted values are all within the 95% confidence interval, which can be seen that the additional momentum method has a better improvement on the back propagation neural networks prediction to accelerate the convergence of the learning process and improve the accuracy of prediction.

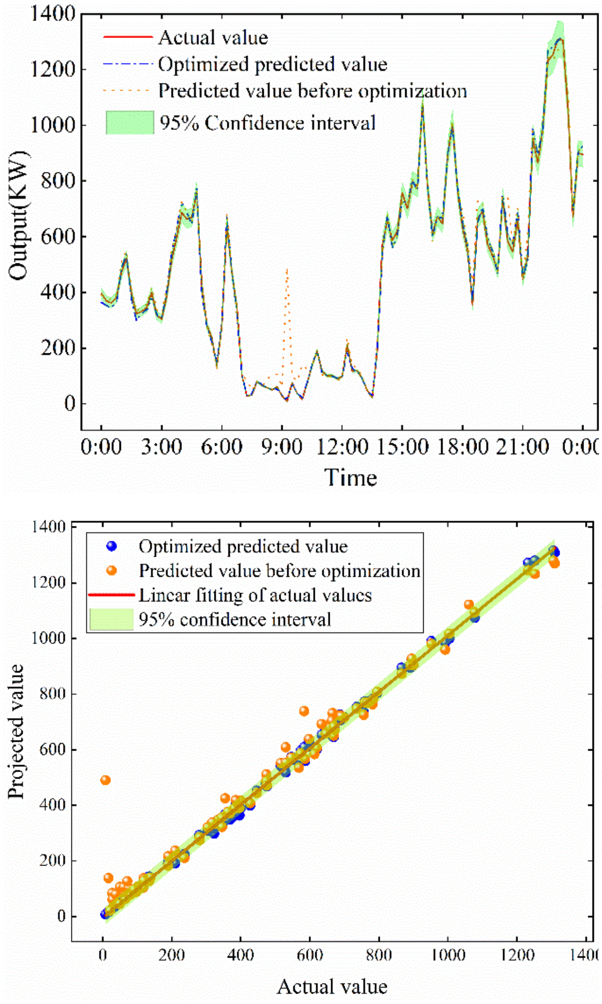

Figure 4. Wind power forecast results

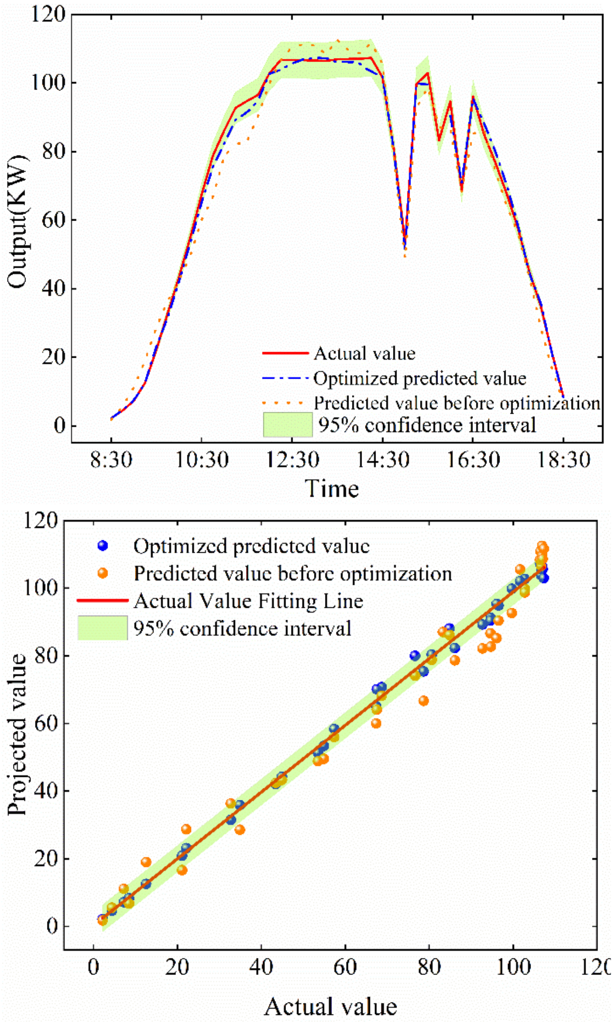

Figure 5. PV forecast results

4.3. System scheduling optimization

In order to analyze the impact of the large amount of wind and photovoltaic power generation intervening in the power system on the optimization results of the virtual power plant scheduling, the tolerance of the system to risk is changed by adjusting the robust coefficients, which are set to 1 (low tolerance), 0.6 (lower tolerance), 0.4 (higher tolerance), and 0.2 (high tolerance), and the choice of robust coefficients can be selected by the scheduling center of the virtual power plant. However, it should be noted that the smaller the robustness coefficient, the higher the utilization of wind power and photovoltaic power generation, a large number of access to the stochastic power generation system will make the virtual power plant's stable and controllable operation is seriously threatened, at the same time, in order to pursue the economy of thermal power generation and to ensure that the basic operation of the output limit, made to reduce the part of the unit operation, as shown in tab. 2.

Table 2. Number of thermal power generation units in operation

Robustness factor	1	0.6	0.4	0.2
Number of units in operation	5	3	2	1

In order to improve the user's electricity consumption habits as a means of smoothing the load curve, the implementation of real-time tariff policy, at the lowest level of impact on the comfort of energy consumption, after 20 times of cyclic regulation to obtain a stable load curve, real-time tariffs at this time as shown in fig. 6.

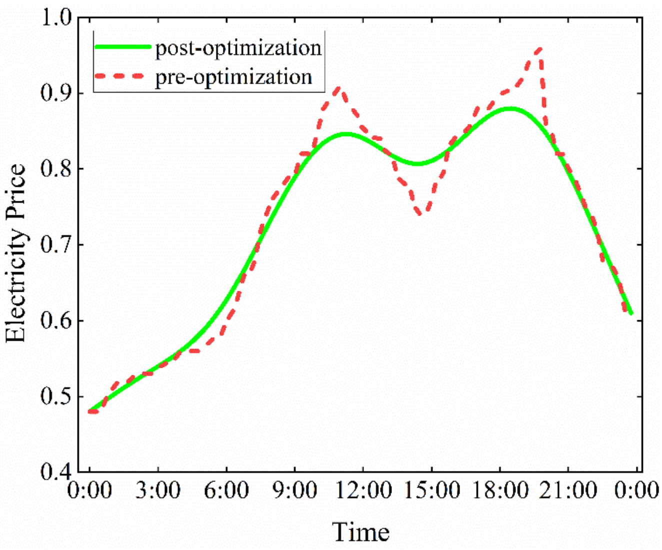

Figure 6. Real-time electricity prices

Thermal and hydro generation curves for a given day are shown in figs. 7 and 8, and due to changing the robustness factor and the number of operating units for thermal generation, the generation efficiency curves for both operations are calculated for better comparison and selection, as shown in figs. 9 and 10. Comparing the two sets of graphs, after increasing the tolerance to risk, the main load task of the system is shifted to hydro, wind and photovoltaic power generation, and thermal power generation is shifted from assuming the main load transfer and pumped storage power plant to assume the peak shifting and frequency shifting tasks at the same time. However, from the operational efficiency diagram, it can be obtained that in the high tolerance, thermal and hydro power generation is always at rated output, when the virtual power plant system to fight against unexpected conditions such as load increase by means of a great limit. However, the utilization of wind and photovoltaic power generation is low at low tolerance, when wind and light abandonment operations are greatly increased and are not realistic.

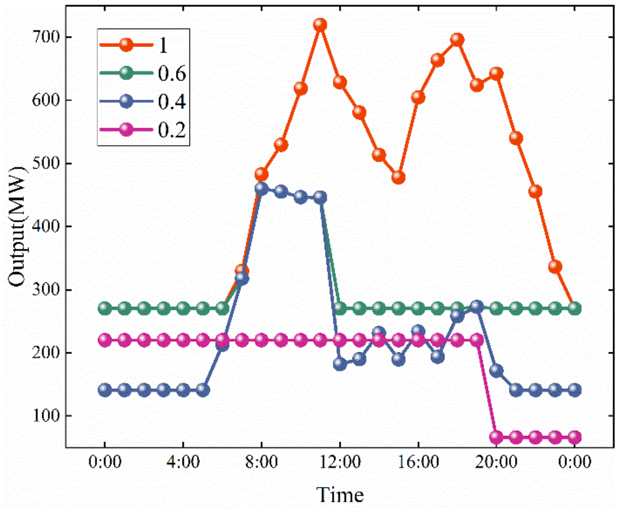

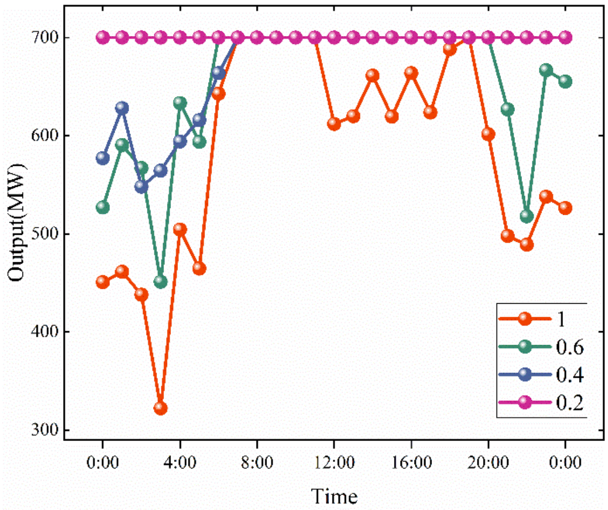

Figure 7. Graph of changes in thermal power plant output

Figure 8. Graph of changes in hydroelectric power plant output

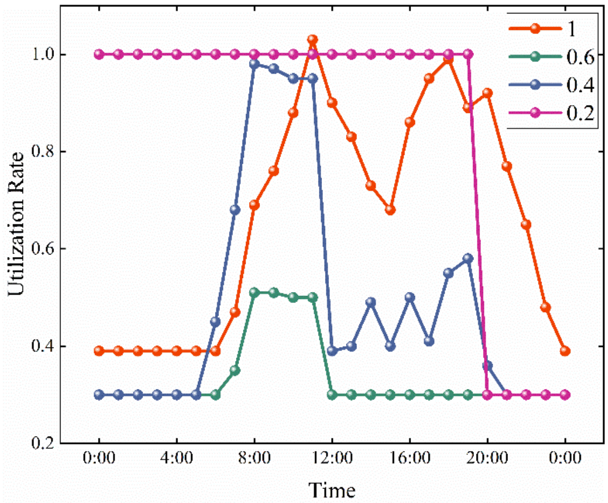

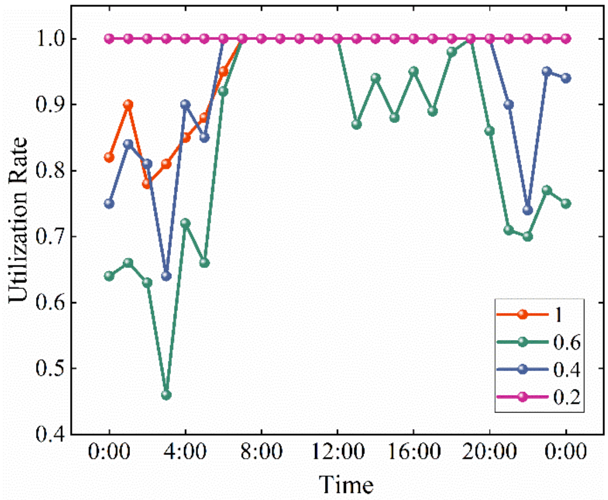

Figure 9. thermal power plant output rate

Figure 10. Hydroelectric power plant output rate

To further investigate the impact of the optimal choice of robustness coefficients on the virtual power plant, the economic efficiency and carbon emissions under different coefficients are predicted and calculated, and fig. 11 and tab. 3 are obtained. Since the cost and carbon emissions of the clean energy generation are lower compared to the thermal power generation, the economic efficiency of the system with a reduced robustness coefficient will increase and the carbon emissions will decrease. However, tab. 3 shows that the economic efficiency when the robustness coefficient is 0.2 is not as high as when it is 0.4, because the robustness coefficient of 0.2 requires a large number of users to store energy to participate in system mobilization, and in the process of constant charging and discharging, the low-priced electricity is stored and the high-priced electricity is released, so that the economic efficiency is not reduced but some of the economic efficiency are transferred to the users who respond positively to the scheduling of the power system. As can be seen from tab. 3 Carbon

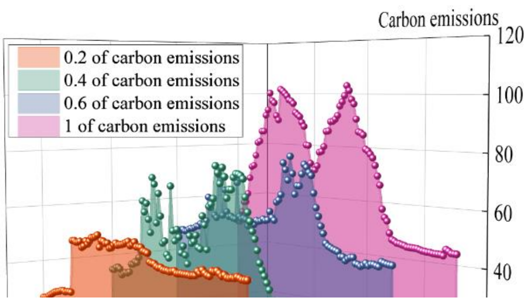

Figure 11 Carbon emissions

Emissions, the largest carbon emissions with a robust coefficient of 1, total emissions of about 6.99 tons, the second largest carbon emissions with a robust coefficient of 0.6, about 5.25 tons, and the carbon emissions with a robust coefficient of 0.4, about 4.6 tons. A robustness factor of 0.2 resulted in the lowest carbon emissions of about 4.22 tons, a reduction of about 40% compared to a robustness factor of 1.

Table 3. Economic efficiency and carbon emissions for different robustness coefficients

Robustness factor	1	0.6	0.4	0.2
Economic benefit (million)	44.75	45.64	45.89	43.82
Carbon footprint (t)	6.99	5.25	4.60	4.22

4.4. Analyze the selection

Comparative analysis of simulation prediction results with different risk tolerances is performed to maximize the economic efficiency and minimize the carbon emissions on the basis of ensuring stable and safe operation of the system. As the robustness coefficient of the virtual power plant decreases with the increase of risk tolerance, the economic efficiency and carbon emissions are close to the optimal. When the system chooses a high-risk tolerance, the economic efficiency reaches 43.82 million and the carbon emission is at least 4.22 tons. However, to implement this plan, the system needs accurate output and load planning, thermal and hydro power generation is at full load for a long time to resist unexpected events is very weak, at the same time, a large number of users need to cooperate with the operation of the virtual power plant, the stability of the operation of the virtual power plant will depend on a larger number of users, which greatly increases the uncertainty. Therefore, choosing a high risk tolerance does not meet the practical significance.

When the system chooses a higher risk tolerance, the economic efficiency and carbon emissions are close to optimal. In this case, the virtual power plant relies on the thermal power generation and energy storage system for FM operation, which ensures that the thermal unit output is within the output limit while leaving part of the output space to resist the risk of sudden load changes. At the same time to ensure the efficient use of wind energy, photovoltaic and hydropower, in terms of social benefits in line with the national "dual-carbon" program, responding to the world's energy development goals.

5. Conclusion

In this study, a Virtual Power Plant (VPP) was organized, which includes wind farms, photovoltaic power plants, hydroelectric power plants, thermal power plants, as well as energy storage devices such as home storage batteries and storage power plants. To investigate the impact of different levels of wind and photovoltaic utilization rates on the VPP, an improved Back Propagation (BP) neural network with additional momentum was first used to predict the output power of wind and photovoltaic generation. A multi-stage adaptive robust optimization control model was then proposed. Four robust coefficients were selected to address the impact of different risk tolerances on the system, and the following conclusions were drawn:

1) The results indicate that the improved prediction method takes less time and achieves higher accuracy, exceeding 95%.

2) The optimal power supply mix for the VPP is a 60% share of renewable energy. At this point, the tolerance is higher. While ensuring the stable operation of the system, a high tolerance does not align with societal needs; a higher tolerance becomes optimal for carbon emissions and economic efficiency. The carbon emissions are 4.60 tons, and the economic efficiency is 45.89 million.

3) The setting of different robustness coefficients reflects the risk tolerance of the VPP. The higher the robustness coefficient, the lower the VPP's risk tolerance, and the less wind and photovoltaic power is incorporated into the system. Incorporating a large amount of wind and solar power under a higher risk tolerance can lead to a weak anti-risk capability of the system and increased likelihood of accidents. Therefore, the risk tolerance of the virtual power plant should not be overly conservative nor overly aggressive.

4) The comparison of the four different robustness coefficients is mainly due to the successive reduction in the number of operating units at thermal power plants and the increased utilization rates of wind and solar energy. It is evident that the reduction in carbon emissions is primarily due to the substitution of renewable energy for traditional energy sources. Therefore, the government should increase its support in terms of technology, funds, and policies for renewable energy.

Acknowledgment

The authors appreciate the financial support by the National Natural Science Foundation of China (Nos. 52069010,51966005).

References

[1] Nenadović S A ,Tekić M Ž,Đorđević M S.ENVIRONMENTALLY-BASED STRUCTURAL DESIGN CRITERIA FOR BUILDINGS. Thermal Science,2018,22(Supplement 4):S1047-S1058. DOI: 10.2298/tsci170525132n

[2] Tan C, et al. Can virtual power plants promote energy transformation—empirical test based on pilot provinces. Energy Reports, 2023, 9: 6135 - 6148. DOI:10.1016/j.egyr.2023.05.023

[3] Wei D , et al. Security region of renewable energy integration: Characterization and flexibility. Energy 187.(2019):115975-115975. DOI: 10.1016/j.energy.2019.115975

[4] Mei S , et al.Optimal bidding strategy for virtual power plant participating in combined electricity and ancillary services market considering dynamic demand response price and integrated consumption satisfaction. Energy 284.(2023): DOI: 10.1016/j.energy.2023.128592

[5] Wang J , et al. Wind speed deterministic forecasting and probabilistic interval forecasting approach based on deep learning, modified tunicate swarm algorithm, and quantile regression. Renewable Energy 179.(2021):1246-1261. DOI: 10.1016/j.renene.2021.07.113

[6] Yildiz C, et al. An improved residual-based convolutional neural network for very short-term wind power forecasting. Energy Conv Manag, 2021, 228. DOI: 10.1016/j.enconman.2020.113731

[7] Cui Y, et al.An algorithm for forecasting day-ahead wind power via novel long short-term memory and wind power ramp events.Energy 263.PC(2023): DOI: 10.1016/j.energy.2022.125888

[8] Wang K, et al. Nonparametric Probabilistic Forecasting for Wind Power Generation Using Quadratic Spline Quantile Function and Autoregressive Recurrent Neural Network. Ieee Transactions on Sustainable Energy, 2022, 13(4): 1930-43. DOI: 10.1109/tste.2022.3175916

[9] Jaseena K.U , et al. Decomposition-based hybrid wind speed forecasting model using deep bidirectional LSTM networks. Energy Conversion and Management 234.(2021).

DOI: 10.1016/j.enconman.2021.113944

[10] Zhao T, et al. Cooperative Optimal Control of Battery Energy Storage System Under Wind Uncertainties in a Microgrid.IEEE Transactions on Power Systems 33.2(2018):2292-2300.

DOI: 10.1109/tpwrs.2017.2741672

[11] Huang Nantian, et al.Combined Probability Prediction of Wind Power Considering the Conflict of Evaluation Indicators.IEEE Access 7.(2019):174709-174724. DOI: 10.1109/access.2019.2954699

[12] Ali G Z, et al. Day-ahead resource scheduling of a renewable energy based virtual power plant.Applied Energy 169.(2016):324-340. DOI: 10.1016/j.apenergy.2016.02.011

[13] Morteza S, et al.An interactive cooperation model for neighboring virtual power plants.Applied Energy 200.(2017):273-289. DOI: 10.1016/j.apenergy.2017.05.066

[14] Rahimiyan M, et al. Strategic Bidding for a Virtual Power Plant in the Day-Ahead and Real-Time Markets: A Price-Taker Robust Optimization Approach. IEEE Transactions on Power Systems: A Publication of the Power Engineering Society 31.4(2016):2676-2687.

DOI: 10.1109/tpwrs.2015.2483781

[15] Tan Z F, et al.Dispatching optimization model of gas-electricity virtual power plant considering uncertainty based on robust stochastic optimization theory.Journal of Cleaner Production 247.(2020):119106-119106. DOI: 10.1016/j.jclepro.2019.119106

[16] Morteza S, et al.The design of a risk-hedging tool for virtual power plants via robust optimization approach.Applied Energy 155.(2015):766-777.

DOI: 10.1016/j.apenergy.2015.06.059

[17] Ana B, et al. Day-Ahead Self-Scheduling of a Virtual Power Plant in Energy and Reserve Electricity Markets Under Uncertainty.IEEE Transactions on Power Systems 34.3(2019):1881-1894.

[18] Hrvoje Pandžić, et al.Offering model for a virtual power plant based on stochastic programming.Applied Energy 105.(2013):282-292. DOI: 10.1016/j.apenergy.2012.12.077

[19] Kardakos, et al. Optimal Offering Strategy of a Virtual Power Plant: A Stochastic Bi-Level Approach.IEEE transactions on smart grid 7.2(2016):794-806. DOI: 10.1109/tsg.2015.2419714

[20] Kara Mostefa Khelil Chérifa, et al.The impact of the ANN’s choice on PV systems diagnosis quality.Energy Conversion and Management 240.(2021). DOI: 10.1016/j.enconman.2021.114278

[21] Feng Y, et al. A short-term load forecasting model of natural gas based on optimized genetic algorithm and improved BP neural network.Applied Energy 134.(2014):102-113.

DOI: 10.1016/j.apenergy.2014.07.104

RECEIVED DATE: 08.01.2024.
DATE OF CORRECTED PAPER: 28.03.2024.
DATE OF ACCEPTED PAPER: 19.04.2024.